PiscoMed Publishing

doi: 10.18282/m.v6i1.597

Original Research Article

Low-cost heterogeneous composite photocatalyst consisting of TiO_2, kaolinite and MMT with improved mechanical strength and photocatalytic activity for industrial wastewater treatment

Pitipanage Pasindu Bhanuka Gunarathne[1], Kohobhange Sujith Prasanna Karunadasa[2,*]

[1] *College of Chemical Sciences, Institute of Chemistry Ceylon, Rajagiriya 10400, Sri Lanka*

[2] *Materials Technology Section, Industrial Technology Institute, Colombo 00700, Sri Lanka*

*** Corresponding author:** Kohobhange Sujith Prasanna Karunadasa, sujith@iti.lk; sujithkohobhange@yahoo.com

Abstract: The industrially feasible TiO_2-clay-based photocatalysts are essential to overcome practical barriers that are inherent to currently available TiO_2-based photocatalysts. The current study demonstrates the fabrication of heterogeneous photocatalyst using TiO_2, kaolinite, and montmorillonite (TKMCP), which has shown improved catalytic activity and mechanical strength, resulting in an industrially feasible photocatalyst. The TKMCP is prepared in a cost-effective manner using 60% TiO_2 and 40% clay with different kaolinite to MMT ratios (1:3 TKMCP1, 1:1 TKMCP2, and 3:1 TKMCP3) by employing mechanical compression and dehydroxylation. The clay ratio predominantly determines the TKMCP mechanical strength and photocatalytic efficiency, where the lowest MMT percentage results in a uniform matrix, in which TiO_2 particles are embedded on clay-sheets. The TKMCP surface became uniform when the MMT percentage is low, whereas a high MMT fraction results in a disordered catalytic surface due to large clay fragments and agglomerates. All three composites accounted for more than 85% of the degradation rate, exhibiting pseudo first order kinetics, resulting in high-rate constants, with the highest observed for TKMCP3, which is 1.55 h^{-1}. The TKMCP3 accounts for the highest mechanical strength, which is 5.83 MPa, while the lowest is observed with TKMCP1, indicating that the TKMCP strength decreases significantly with high MMT fraction. TKMCP has several advantages, including easy fabrication, low cost, free of hazardous chemicals, high production capacity with minimal machinery/supervision, non-self-degradability, easy disposal, easy installation in pilot-scale reactors, compatibility with both batch and flow reactors, environmental, and user-friendliness. TKMCP can also be obtained in variable sizes and shapes that ensure dynamic wastewater treatment applications.

Keywords: TiO_2; kaolinite; MMT; composite photocatalyst; industrial wastewater treatment

Received: 11 September 2023; **Accepted:** 12 October 2023; **Available online:** 10 November 2023

1. Introduction

The efficient wastewater treatment has been a controversial issue that grows rapidly across the globe, mainly due to industrialization, growing demand for drinkable water, and environmental pollution[1]. The agrochemical and industrial wastes are the major pollutants that need effective remediation via conversion to harmless end products, meeting the stipulated disposal standards. The industrial wastewater treatment is often carried out by the alkaline hydrolysis method, where high alkaline consumption itself is a problem when considering high material costs, low treatment efficacy, alkaline disposal, etc.[1].

Titanium dioxide (TiO_2) is a well-known multifunctional semiconductor photocatalyst, the catalytic activity of which is mainly achieved via advance oxidation, where organic waste decontamination is initiated by electron-hole pair generation under sunlight/UV irradiation and is often used to mineralize a variety of organic pollutants in wastewater into harmless end products, including carbon dioxide, water, and inorganic ions[2]. In addition to alkaline hydrolysis, direct use of TiO_2 powder is often employed in general practice. This method, however, has a number of drawbacks, including low efficiency and ineffective post-separation[2]. The direct use of TiO_2 powder has been no longer feasible due to practical barriers; in contrast, immobilization techniques are known to have potential advantages over powder application[3]. The immobilized systems rather accounted for higher surface area, superior adsorption properties, and increased surface hydroxyl groups or reduced charge recombination[4].

The photocatalyst immobilization can be achieved on different substrates. The well-known examples are powder/pellet, soft/thin, and rigid substrates[2]. The activated carbon, clay, and volcanic ash are the better powder/pellet substrates that are often used to immobilize photocatalysts[5,6]. Alumina, polyvinylidene difluoride, glass filters, cellulose fibers, and sponges are the well-known examples for soft/thin substrates[7–10]. The glass surfaces most of the time act as rigid substrates that are used to immobilize photocatalysts, mainly by incorporating organic/inorganic binders[4].

TiO_2 immobilization on a substrate can be accomplished through two main strategies: using binders or physically anchoring TiO_2 particles on the substrate[1]. The immobilization using organic/inorganic binders, including polyester resin, polyethylene, polypropylene, polyethylene glycol, and silicon adhesive, accounts for a poor TiO_2 immobilization[11–13]. The binders are typically organic in nature, making them highly susceptible to self-degradation (by TiO_2) under irradiation of sun/UV light. Conversely, TiO_2 particles can submerge and agglomerate inside the binder, which ultimately results in a diminishing photocatalytic activity. The coating preparation is also imperfect and complex, which makes it difficult to maintaining the uniformity and durability. The photocatalytic efficiency and coating stability/durability are reasonably decreased due to submerged TiO_2 particles inside the binder and self-degradation of binder, respectively.

Apart from binder-based immobilization, clay is better supportive substrate among many types available, which often used to anchor the photocatalysts to the clay surface, making it a promising raw material for hybrid photocatalysts. TiO_2-clay photocatalysts are diversified with respect to both preparation and morphology[1]. The sol-gel process has been widely used to produce clay-based photocatalysts that involve growing and anchoring of nanosized TiO_2 particles on the clay surface. However, these clay-based products are mainly in powder/particles/aggregates forms, which makes commercial applications less feasible due to constraints associated with the implementation of large-scale reactors. Major limitations of existing TiO_2-clay-based photocatalysts are high manufacturing costs, post-separation issues, short-term durability, and installation difficulties, particularly in large industrial treatment tanks[1]. It has also been discovered that TiO_2-based photocatalyst technology available is less feasible and even fails to address real industrial requirements/capacity when it comes to wastewater treatment[13,14].

To overcome the drawbacks that are linked to existing photocatalysts, a novel approach is required to prepare a dynamic photocatalyst, which can easily integrate with commercial wastewater treatment units. This will be achieved by utilizing the knowledge of clay-based composite materials that were previously prepared by chemical-free synthesis path in which only mechanical compression and heat treatment are employed. Mechanical compression is decisive in material engineering because it can create novel structural elements that result in improved material properties. In the present work, a similar technical approach is employed to

fabricate a novel TiO_2-kaolinite-MMT composite photocatalyst (TKMCP), making the material highly photocatalytic and industrially feasible.

2. Material and methods

2.1. Materials

TiO_2 (Degussa P25 powder, 56 nm particles) was obtained from Nippon Aerosil Co. Ltd., Japan. The kaolinite (>99%, 1.2 μm particles), MMT clay (>99%, average particle size 4.5 μm), and methylene blue (>99%) were acquired from Sigma-Aldrich Ltd., USA.

2.2. TKMCP blocks fabrication

To fabricate composite suspensions, a fixed amount of TiO_2 (60%) was mixed in distilled water with various clay (in total 40%) ratios and then continuously stirred at 1000 rpm for 3 h with an overhead agitator (IKA, Germany). TKMCP1, TKMCP2, and TKMCP3 were prepared in 25 g by combining kaolinite and MMT in the ratio of 1:3, 1:1, and 3:1 by weight (%w). TKMCP blocks with dimensions of 4 cm × 4 cm × 0.8 cm were prepared by applying a 125,000 N vertical ram force to a partially dried composite material that was uniformly packed inside a specially designed steel mould for 30 min. TKMCP blocks were then calcined in a high-temperature furnace (Nebertherm) for 45 min at 650 ℃, which results in TiO_2-laolinite-MMT heterogeneous photocatalyst (**Figure 1**). The photocatalytic activity was measured using modified TKMCP blocks with an untreated top surface. To achieve this, the side and bottom surfaces of TKMCP blocks were uniformly painted, with the exception of the top surface, which serves as the active exterior, facilitating photocatalytic disintegration.

Figure 1. Major steps employed in TKMCP blocks fabrication.

2.3. TKMCP blocks characterization

X-ray diffractometer (Rigaku Ultima IV, Japan) equipped with a copper target X-ray generator ($\lambda_{CuK\alpha1}$—0.154056 nm), a secondary beam curved graphite monochromator, and a D/tex Ultra detector was used to analyze the TKMCP blocks and raw materials. The powdered samples were analyzed using an X-ray beam

generated under standard tube conditions, which included a 40 kV tube voltage and a current of 30 mA. To obtain diffractograms, the samples were scanned between 10° and 130° at 2° min^{-1}. The X-ray beam geometry was meticulously optimized, with the divergence slit, scattering slit, and receiving slit all fine-tuned by 2/3°, 2/3°, and 0.45 mm, respectively. The Rietveld refinement on XRD profiles was carried out with the help of an advanced WPPF (whole powder pattern fitting) component that interfaced with the PDXL integrated X-ray powder diffraction software. The refined diffractograms were analyzed using PDXL integrated X-ray powder diffraction software, which was linked to the ICDD database (International Centre for Diffraction Data). The Spur and Myers equation, which describes the relationship between peak intensity and weight fraction of anatase, x_A, was used to determine the TiO_2 composition in each composite (Equation (1))[15,16].

$$x_A = \frac{0.79I_{A(101)}}{(I_{R(110)} + 0.79I_{A(101)})} \quad (1)$$

where $I_{A(101)}$ and $I_{R(110)}$ denote the intensity of the strongest anatase (25.30°) and rutile (27.37°) reflections, respectively.

The flexural strength was calculated by substituting the force of rupture, which was determined using the TKMCP strips (universal testing machine, Testometric, UK)[17]. To achieve this, the TKCMP strip was carefully placed horizontally on the supporting stage of the Testometric universal testing machine, and the force at the fracture point was measured upon collision with a load that moved vertically at a rate of 2 mm min^{-1}.

$$\sigma_f = \frac{FL}{2bd^2} \quad (2)$$

where σ_f, F, L, b, and d stand for flexural strength, force at fracture point, supporting span length (2.00 cm), width (1.3 cm), and depth (0.8 cm) of TKCP strip, respectively.

A scanning electron microscope (ZEISS EVO LS15, Germany) was used to examine the TKMCP series, yielding well-resolved images at a constant accelerating voltage of 20 kV. The FT-IR spectra were collected with a Bruker Tensor 27 spectrometer (Germany) in an attenuation total reflection module (ATR) with a diamond puck (sample compartment). The samples were scanned at a resolution of 4 cm^{-1} between 600 and 4000 cm^{-1}, yielding a transmittance spectrum from which the vibration frequencies corresponding to IR bands were obtained. The thermal profile and stability of clay minerals were initially determined by TGA/DSC analysis (TA instruments SDTQ600, USA).

2.4. TKMCP photocatalytic activity determination

The modified TKMCP was used in a photocatalytic degradation study, in which the degradation of methylene blue solution in the presence of TKMCP was measured using a UV-1800 Shimadzu UV-Visible spectrophotometer (Japan, λ_{max} = 664 nm). The reaction vessels used in photocatalytic degradation studies were made by placing each TKMCP block inside a crystallization flask (150 mL) and then adding 100 mL of methylene blue solution (1.56×10^{-5} mol dm^{-3}). The reaction vessels were then exposed to sunlight for 2.5 h, with absorbance measurements taken at every 30 min interval to determine the rate of methylene blue degradation over time. The concentration of dye after each successive irradiation was determined using a calibration plot constructed with known concentrations of methylene blue solutions. The UVProbe software, which is integrated with the UV-Vis spectrophotometer, was used to construct the calibration plot. The concentration of the irradiated samples was determined directly from the previously installed calibration plot. The entire experiment was carried out in natural sunlight, with an average irradiation (intensity) of 425 W m^{-2}. The average temperature during the entire sample irradiation was 30.5 °C, which corresponds to the daytime

average temperature. The percentage degradation (D) and the pseudo first-order rate constant (k) were determined employing the following relationships after determining methylene blue concentration with respect to the control sample[18].

$$D = \frac{C_0 - C_{MB}}{C_0} \times 100\% \quad (3)$$

$$\ln C_{MB} = -kt + \ln C_0 \quad (4)$$

where C_0 (1.56×10^{-5} mol dm^{-3}), C_{MB}, and t denote the initial concentration of methylene blue, concentration at time t, and time, respectively.

3. Results and discussion

The composite photocatalyst is prepared using both clay types instead of single clay because preliminary studies revealed that combined clay can significantly improve mechanical strength. According to initial studies, TiO_2 amount that can effectively be incorporated into TKMCP is found to be around 60%, greater than which the composite stability is drastically reduced, causing multiple surface cracks. Therefore, the maximum clay amount that can be incorporated into TKMCP is restricted to 40%. The clay dehydroxylation is initially observed by TGA/DTA analysis, which indicates that both clay types undergo complete dehydroxylation at elevated temperatures (**Figure 2**). The kaolinite dehydroxylation is rapidly occurring at 500 °C in a single step process, which clearly reflects in both thermograms, resulting in a considerable weight loss according to TGA (**Figure 2(a)**). Unlike kaolinite, the dehydroxylation of MMT takes place in two steps, where the first and second dehydroxylation occur at 500 °C and 645 °C, respectively. Therefore, the firing temperature should be set somewhere above 645 °C, which ensures effective dehydroxylation of both clays. This explains why 650 °C was chosen as the firing temperature for composite fabrication.

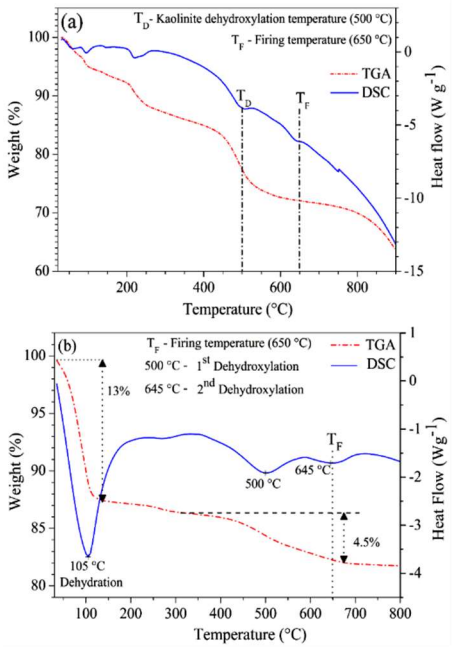

Figure 2. TGA-DSC of **(a)** Kaolinite; **(b)** MMT.

Despite the fact that the anatase to rutile transition is more likely to occur at low temperatures, XRD analysis of TKCP reveals that the composition changes insignificantly during dehydroxylation (**Table 1**). The authors of current article revealed that the same TiO_2 powder underwent a measurable phase transition

relatively at low temperatures, resulting in a composition change of ~25% at 650 ℃[16]. The most likely explanation for avoiding such a change in the present work is that clay dehydroxylation occurred predominantly during phase transformation, preventing anatase to rutile conversion at dehydroxylation temperature. The clay matrix acts as a barrier against phase transformation, ensuring unharmed photocatalytic activity of TiO_2. Clay matrix not only serves as a phase transition barrier but is also incorporated into the architectural framework of composites, improving matrix strength and stability.

Table 1. TKMCP composition.

Composite	**Composition (%)**	
	Anatase	**Rutile**
	(00-084-1285)	**(00-078-1508)**
Raw TiO_2	81.0	19.0
TKMCP1	78.7	21.3
TKMCP2	80.6	19.4
TKMCP3	80.7	19.3

Database card numbers are given in the parenthesis.

The characteristic clay IR bands, which are shown in **Figure 3**, are absent in the respective TKMCP FT-IR spectra, confirming the complete dehydroxylation. The typical kaolinite IR vibration bands (in plane Si-O stretching vibration at 1114 cm^{-1} and 1007 cm^{-1}, OH vibration of inner and outer Al-OH bonds at 912 cm^{-1}) are clearly absent in TKMCP, indicating complete kaolinite dehydroxylation, which results in a clay amorphization (**Figure 3**)[19,20]. However, the broad Ti-O stretching vibration band, which appears between 900 cm^{-1} and 600 cm^{-1} can mask characteristic kaolinite Si-O-Al stretching bands at 788 cm^{-1} and 748 cm^{-1}. Therefore, the confirmation of clay dehydroxylation based on such kaolinite IR bands is somewhat less reliable. The MMT IR bands, which typically appear at 1110 cm^{-1} and 986 cm^{-1} for Si-O stretching and 910 cm^{-1} for Al-OH, are also absent in TKMCP, indicating MMT dehydroxylation. The newly emerging amorphous SiO_2 IR-band (anti-symmetric Si-O stretching) at 1035 cm^{-1} and the disappearance of hydroxyl stretching/bending IR bands that are typically observed at 3689, 3619, 1631, and 1407 cm^{-1} for kaolinite and 3618, 1634, and 1404 cm^{-1} for MMT also ensure complete clay dehydroxylation[19,20] (**Figure 3**).

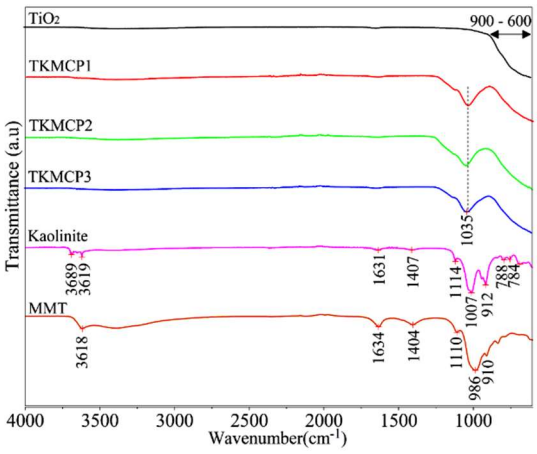

Figure 3. FT-IR spectra of raw materials and composites.

TKMCP composites are negative for characteristic XRD clay peaks, resulting in broad amorphous kaolinite and MMT peaks, which are also in better agreement with FT-IR outcomes, confirming the complete

clay amorphization due to dehydroxylation (**Figures 4** and **5**). Despite the amorphous nature, the heated clay materials retained some of the structural characteristics of raw clay, which results in a short-range ordered material to some extent[21–23]. In crystallography, the regular arrangement of atoms over a short distance in the absence of a periodic array refers to a short-range order[21,22]. The broad X-ray peaks related to clay result from these short-range ordered constituents. Such broad peaks typically indicate very poor crystallinity, resulting in a small grain size.

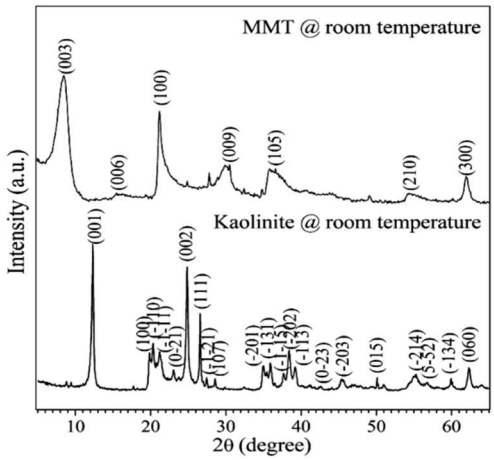

Figure 4. X-ray diffractograms of raw kaolinite and MMT (Miller indices are given in the parenthesis).

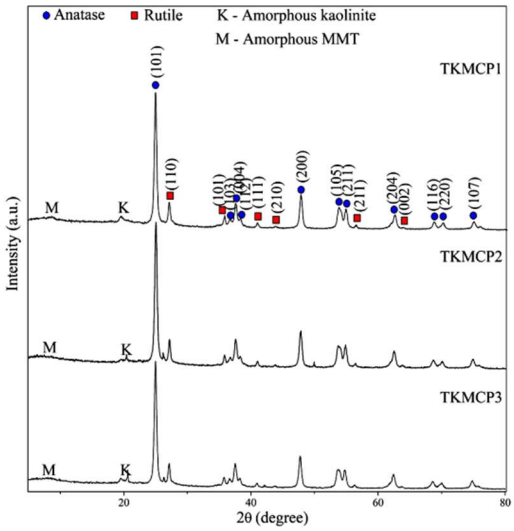

Figure 5. X-ray diffractograms of TKMCP series, exhibiting the amorphization of clay due to dehydroxylation (Miller indices of anatase and rutile are given in the parenthesis).

TKMCP is a potential photocatalyst, the photocatalytic activity and mechanical strength of which are crucial for determining industrial level feasibility. TKMCP photocatalytic activity is determined by percentage degradation, which increases slightly from TKMCP1 to TKMCP3 after 2.5 h of sunlight exposure (**Table 2**). Methylene blue concentration is rapidly decreased with time, which indicates all the composite photocatalysts have better catalytic activity, resulting in rapid dye disintegration (**Figure 6**). The photocatalytic activity of TKMCP alone is insufficient to determine whether the composite is suitable for commercial application; mechanical strength also plays an important role in this regard. Mechanical strength increases in a similar manner, with TKMCP3 exhibiting the highest flexural strength (**Table 2**).

Table 2. Methylene blue degradation efficiency, kinetic parameters and flexural strength of TKMCP.

Composite photocatalyst	Parameter		
	MB degradation (%)	**σ_f (MPa)**	**k (h^{-1})**
TKMCP1	86.9	3.57	1.25
TKMCP2	90.9	4.42	1.32
TKMCP3	91.0	5.83	1.55

k—pseudo first order rate constant, σ_f—flexural strength, MB—methylene blue.

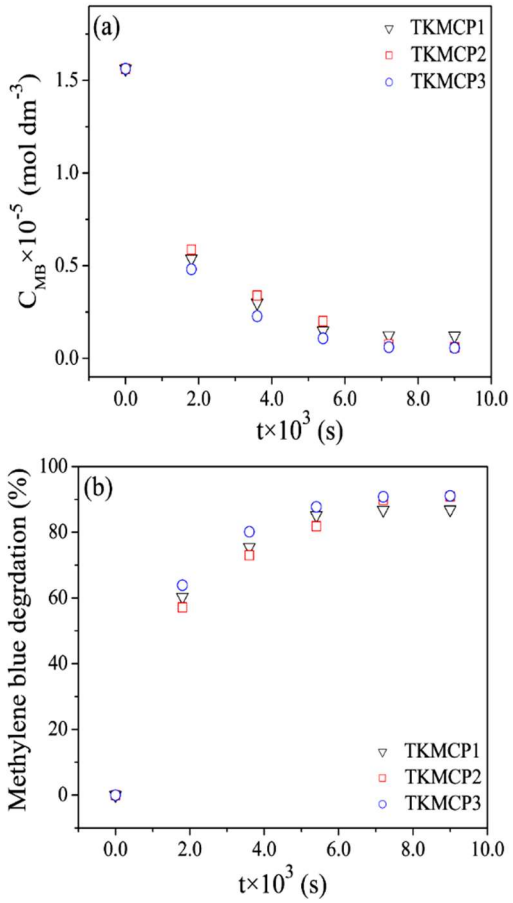

Figure 6. TKMCP efficiency in methylene blue degradation as a function of time **(a)** MB concentration (C_{MB}—methylene blue concentration); **(b)** % dye degradation (calculated by Equation (3)).

The methylene blue degradation on TKMCP follows pseudo first order kinetics under sunlight irradiation, with a gradual increase in rate constant with increasing kaolinite percentage (**Figure 7(a)** and **Table 2**). The linear relation that has been observed with ln C as a function of time reveals the first order kinetics, where C and 1/C clearly result in a non-linear correlation with time (**Figure 6(a)** and **Figure 7(b)**). The rate constants determined with TKMCP are greater than those of many photocatalysts tested against methylene blue, including TiO_2 nanotrees (0.346 h^{-1}), TiO_2 nanobelts (0.026 h^{-1}), and multilayer TiO_2 coating on HDPE (0.27–0.43 h^{-1})[24–26]. As the rate constant increased, the time taken for complete dye disintegration became shorter, which is very crucial for industrial wastewater treatment because it results in a considerable reduction in both time and cost. TKCMP internal matrix, which is responsible for better functioning of the composite, needs an in-depth analysis that is essential to understanding the structure-property correlations. Therefore, SEM micrographs were examined with great care, observing structure-property correlations that are essential to predicting the photocatalytic activity and the reaction kinetics related to TKMCP.

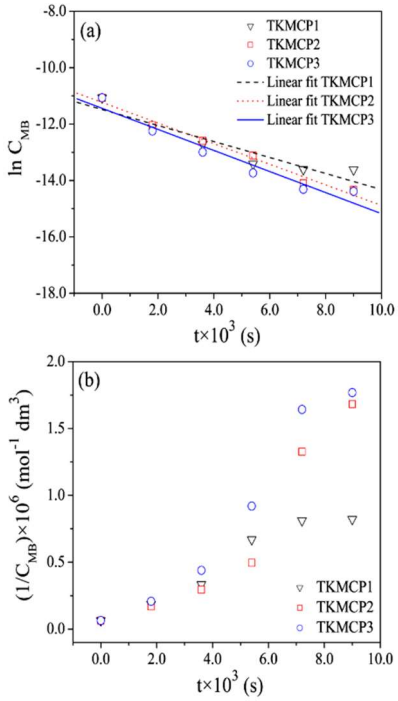

Figure 7. Methylene blue degradation kinetics on TKMCP under sunlight irradiation **(a)** ln C_{MB} vs. time; **(b)** $1/C_{MB}$ vs. time.

Mechanical compression is used to fabricate TKMCP, resulting in a highly compressed clay matrix embedded with TiO_2 particles (**Figure 8**). The authors of the current study previously reported the formation of tiny clay particles during the fabrication of graphite-clay composite electrodes using a similar technique[27–29]. However, even with the same fabrication technique, the outcomes of the current study are significantly different, resulting in clay sheets rather than tiny particles. This is evident in TKMCP SEM micrographs, in which TiO_2 particles embedded in clay matrix can clearly be observed with the composite consisting of low MMT fraction (**Figure 8**).

The number of TiO_2 particles available on the surface, the strength of TiO_2-clay interactions, and the number of surface defects are likely to determine the strength and photocatalytic efficiency of TKMCP. The TKMCP with the lowest MMT percentage produces uniform clay layers, whereas the TKMCP with a high MMT percentage disrupts the uniformity, which results in a highly disordered matrix containing large clay fragments. As the MMT percentage decreases, the surface defects gradually decrease, resulting in a TiO_2 particle embedded in a continuous, uniform sheet-like clay matrix with insignificant surface defects that can be seen when moving from TKMCP1 to TKMCP3. The thin clay layers can accommodate a large number of tiny TiO_2 particles, which are most likely interacted by dehydroxylation via the Ti-O-Si and Al-O-Ti bonds, resulting in negligible surface defects[30].

The high MMT amount is likely responsible for clay agglomeration, which caused poor pilling of clay under mechanical compression, resulting in a significant number of surface defects. Furthermore, TiO_2 particles can become trapped within these large clay agglomerates, limiting their availability on the composite surface and significantly effects on catalytic activity and mechanical strength. Because particle agglomeration reduces the effective clay-TiO_2 interactions, TKMCP with a high MMT fraction has significantly low mechanical strength (**Table 2**). In contrast, TKMCP has a relatively large surface area, mechanical strength, and photocatalytic activity with low MMT fraction. This explains why TKMCP3 has a comparatively higher rate constant due to a less disordered catalytic surface. The internal TKMCP structure became more uniform and consisting of fewer defects with the lowest MMT percentage, as seen in the SEM micrographs (**Figure**

8(c)). Such matrix with low surface defects accounts for the improved photocatalytic activity and mechanical strength that are observed in TKMCP3 (**Table 2**).

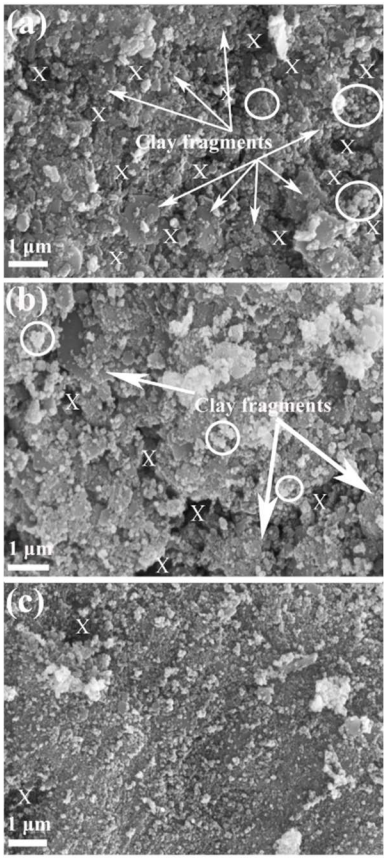

Figure 8. SEM images exhibiting TKMCP surface **(a)** TKMCP1; **(b)** TKMCP2; **(c)** TKMCP3.

When going from TKMCP1 to TKMCP3, the surface defects (marked by an "X") and agglomerates (TiO_2 incorporated clay clusters, marked by circles) are gradually reduced. A uniform sheet-like clay matrix that is highly embedded with TiO_2 particles is observed in TKMCP3 with the lowest MMT percentage instead of large clay fragments, which are more prominent in TKMCP1 with higher MMT fraction. TiO_2 particles appeared as small spots (bright), which are scattered throughout the entire clay surface (dark in color). A very high TiO_2 particle concentration can also be observed in TKMCP3 compared to TKMCP1, resulting in the highest photocatalytic efficacy.

TKMCP composite photocatalysts, unlike many TiO_2 based photocatalysts on the market, can be fabricated in a variety of shapes and sizes using a low-cost fabrication method that requires little labor, machinery, and inexpensive raw materials. TKMCP is simple to implement in large-scale industrial wastewater treatment plants that use renewable sunlight or UV radiation. Another advantage of TKMCP over powder type photocatalysts is the lack of post-separation, which ensures long-term reusability. The TKMCP is a better product that bridges the gap between lab-scale and industrial-scale wastewater treatment units.

4. Conclusions

A simple method is used to fabricate an industrially feasible TiO_2-kaolinite-MMT composite photocatalyst, which consists of inexpensive raw materials. The fabrication route is designed to avoid additional reagents, making the process more cost-effective, faster, and environmentally friendly. The TKMCP

can be manufactured in a variety of shapes and sizes to match the reactor dimensions, reducing engineering constraints when upgrading the lab-scale product to pilot-scale reactors. The TKMCP's physical properties are primarily determined by the clay type and amount incorporated, with the lowest MMT percentage resulting in better performance. The TKMCP3 photocatalytic activity and flexural strength are comparatively high, exhibiting the highest first-order rate constant. This is mainly due to tiny TiO_2 particles embedded in clay sheet-like arrangement, which accounts for an insignificant amount of clay fragments and agglomerates. In contrast, TKMCP1 has comparatively low flexural strength and photocatalytic activity, which is primarily due to a disordered matrix resulting from large clay fragments and agglomerates. The future implementations, including mechanical strength enhancement and converting TKMCP to absorb visible light, can be achieved via incorporation of additional mineral phases and TiO_2 doping, respectively. The TiO_2 immobilization technique described here is very useful for large-scale commercial fabrication of photocatalysts aimed at high-capacity wastewater treatment plants powered by renewable sunlight or UV irradiation. The simple chemical-free fabrication process makes commercial-level TKMCP production more feasible with minimal supervision and machinery that ultimately results in a high production output.

Author contributions

Conceptualization, KSPK; methodology, KSPK; software, PPBG and KSPK; validation, KSPK; formal analysis, PPBG; investigation, PPBG and KSPK; resources, KSPK; data curation, PPBG and KSPK; writing—original draft preparation, PPBG and KSPK; writing—review and editing, KSPK; visualization, KSPK; supervision, KSPK; project administration, KSPK; funding acquisition, KSPK. All authors have read and agreed to the published version of the manuscript.

Funding

The financial support for this research is provided by the National Research Council of Sri Lanka under grant number 20-014.

Conflict of interest

The authors have no competing interests to declare that are relevant to the content of this article.

References

1. Szczepanik B. Photocatalytic degradation of organic contaminants over clay-TiO_2 nanocomposites: A review. *Applied Clay Science* 2017; 141: 227–239. doi: 10.1016/j.clay.2017.02.029
2. Lazar AM, Varghese S, Nair SS. Photocatalytic water treatment by titanium dioxide: Recent updates. *Catalysts* 2012; 2(4): 572–601. doi: 10.3390/catal2040572
3. Shan AY, Ghazi TIM, Rashid SA. Immobilisation of titanium dioxide onto supporting materials in heterogeneous photocatalysis: A review. *Applied Catalysis A: General* 2010; 389(1–2): 1–8. doi: 10.1016/j.apcata.2010.08.053
4. Stathatos E, Papoulis D, Aggelopoulos CA, et al. TiO_2/palygorskite composite nanocrystalline films prepared by surfactant templating route: Synergistic effect to the photocatalytic degradation of an azo-dye in water. *Journal of Hazardous Materials* 2012; 211–212: 68–76. doi: 10.1016/j.jhazmat.2011.11.055
5. Esparza P, Borges ME, Díaz L, et al. Photodegradation of dye pollutants using new nanostructured titania supported on volcanic ashes. *Applied Catalysis A: General* 2010; 388(1–2): 7–14. doi: 10.1016/j.apcata.2010.07.058
6. Zhu B, Zou L. Trapping and decomposing of color compounds from recycled water by TiO_2 coated activated carbon. *Journal of Environmental Management* 2009; 90(11): 3217–3225. doi: 10.1016/j.jenvman.2009.04.008
7. Djafer L, Ayral A, Ouagued A. Robust synthesis and performance of a titania-based ultrafiltration membrane with photocatalytic properties. *Separation and Purification Technology* 2010; 75(2): 198–203. doi: 10.1016/j.seppur.2010.08.001
8. Damodar RA, You SJ, Chou HH. Study the self cleaning, antibacterial and photocatalytic properties of TiO_2 entrapped PVDF membranes. *Journal of Hazardous Materials* 2009: 172(2–3): 1321–1328. doi:

10.1016/j.jhazmat.2009.07.139
9. Liu L, Liu Z, Bai H, Sun DD. Concurrent filtration and solar photocatalytic disinfection/degradation using high-performance Ag/TiO_2 nanofiber membrane. *Water Research* 2012; 46(4): 1101–1112. doi: 10.1016/j.watres.2011.12.009
10. Bedford NM, Pelaez M, Han C, et al. Photocatalytic cellulosic electrospun fibers for the degradation of potent cyanobacteria toxin microcystin-LR. *Journal of Materials Chemistry* 2012; 22: 12666–12674. doi: 10.1039/C2JM31597A
11. Tennakone K, Tilakaratne CTK, Kottegoda IRM. Photocatalytic degradation of organic contaminants in water with TiO_2 supported on polythene films. *Journal of Photochemistry and Photobiology A: Chemistry* 1995; 87(2): 177–179. doi: 10.1016/1010-6030(94)03980-9
12. Tennakone K, Kottegoda IRM. Photocatalytic mineralization of paraquat dissolved in water by TiO_2 supported on polythene and polypropylene films. *Journal of Photochemistry and Photobiology A: Chemistry* 1996; 93(1): 79–81. doi: 10.1016/1010-6030(95)04141-9
13. Kumara GRRA, Sultanbawa FM, Perera VPS, et al. Continuous flow photochemical reactor for solar decontamination of water using immobilized TiO_2. *Solar Energy Materials and Solar Cells* 1999; 58(2): 167–171. doi: 10.1016/S0927-0248(98)00200-1
14. Tennakone K, Tilakaratne CTK, Kottegoda IRM. Photomineralization of carbofuran by TiO_2-supported catalyst. *Water Research* 1997; 31(8): 1909–1912. doi: 10.1016/S0043-1354(97)00031-6
15. Spurr RA, Myers H. Quantitative analysis of anatase-rutile mixtures with an X-ray diffractometer. *Analytical Chemistry* 1957; 29(5): 760–762. doi: 10.1021/ac60125a006
16. Karunadasa KSP, Manoratne CH. Microstructural view of anatase to rutile phase transformation examined by in-situ high-temperature X-ray powder diffraction. *Journal of Solid State Chemistry* 2022; 314: 123377. doi: 10.1016/j.jssc.2022.123377
17. Temenoff JS, Mikos AG. *Biomaterials: The Intersection of Biology and Materials Science*, 1st ed. Pearson prentice Hall; 2008.
18. Alkaykh S, Mbarek A, Ali-Shattle EE. Photocatalytic degradation of methylene blue dye in aqueous solution by $MnTiO_3$ nanoparticles under sunlight irradiation. *Heliyon* 2020; 6: e03663. doi: 10.1016/j.heliyon.2020.e03663
19. Kutláková MK, Tokarský J, Kovář P, et al. Preparation and characterization of photoactive composite kaolinite/TiO_2. *Journal of Hazardous Materials* 2011; 188(1–3): 212–220. doi: 10.1016/j.jhazmat.2011.01.106
20. Sengyang P, Rangsriwatananon K, Chaisena A. Preparation of zeolite N from metakaolinite by hydrothermal method. *Journal of Ceramic Processing Research* 2015; 16(1): 111–116.
21. Meng Y, Gong G, Wei D, Xie Y. In situ high temperature X-ray diffraction study on high strength aluminous porcelain insulator with the Al_2O_3-SiO_2-K_2O-Na_2O system. *Applied Clay Science* 2016; 132–133: 760–767. doi: 10.1016/j.clay.2016.07.014
22. Chakraborty AK. DTA study of preheated kaolinite in the mullite formation region. *Thermochimica Acta* 2003; 398(1–2): 203–209. doi: 10.1016/S0040-6031(02)00367-2
23. De Aza AH, Turrillas X, Rodriguez MA, et al. Time-resolved powder neutron diffraction study of the phase transformation sequence of kaolinite to mullite. *Journal of the European Ceramic Society* 2014; 34(5): 1409–1421. doi: 10.1016/j.jeurceramsoc.2013.10.034
24. Kasanen J, Salstela J, Suvanto M, Pakkanen TT. Photocatalytic degradation of methylene blue in water solution by multilayer TiO_2 coating on HDPE. *Applied Surface Science* 2011; 258(5): 1738–1743. doi: 10.1016/j.apsusc.2011.10.028
25. Al-Rawashdeh NAF, Allabadi O, Aljarrah MT. Photocatalytic activity of graphene oxide/zinc oxide nanocomposites with embedded metal nanoparticles for the degradation of organic dyes. *ACS Omega* 2020; 5(43): 28046–28055. doi: 10.1021/acsomega.0c03608
26. Dharma HNC, Jaafar J, Widiastuti N, et al. A review of titanium dioxide (TiO_2)-based photocatalyst for oilfield-produced water treatment. *Membranes* 2022; 12(3): 345. doi: 10.3390/membranes12030345
27. Karunadasa KSP, Manoratne CH, Pitawala HMTGA, Rajapakse RMG. A potential working electrode based on graphite and montmorillonite for electrochemical applications in both aqueous and molten salt electrolytes. *Electrochemistry Communications* 2019; 108: 106562. doi: 10.1016/j.elecom.2019.106562
28. Karunadasa KSP, Rathnayake D, Manoratne C, et al. A binder-free composite of graphite and kaolinite as a stable working electrode for general electrochemical applications. *Electrochemical Science Advances* 2021; 1(4): e2100003. doi: 10.1002/elsa.202100003
29. Rathnayake DT, Karunadasa KSP, Wijekoon ASK, et al. Low-cost ternary composite of graphite, kaolinite and cement as a potential working electrode for general electrochemical applications. *Chemical Papers* 2022; 76: 6653–6658. doi: 10.1007/s11696-022-02314-w
30. Dlamini MC, Maubane-Nkadimeng MS, Moma JA. The use of TiO_2/clay heterostructures in the photocatalytic remediation of water containing organic pollutants: A review. *Journal of Environmental Chemical Engineering* 2021; 9(6): 106546. doi: 10.1016/j.jece.2021.106546